



Published in final edited form as:

J Am Chem Soc. 2009 August 5; 131(30): 10497–10506. doi:10.1021/ja902694n.

Binding and Inactivation Mechanism of a Humanized Fatty Acid Amide Hydrolase by α -Ketoheterocycle Inhibitors Revealed from Co-Crystal Structures

Mauro Mileni[†], Joie Garfinkle^{§,#}, Jessica K. DeMartino^{§,#}, Benjamin F. Cravatt^{‡,#,*}, Dale L. Boger^{§,#,*}, and Raymond C. Stevens^{†,§,*}

[†] Department of Molecular Biology, The Scripps Research Institute, 10550 North Torrey Pines Road, La Jolla, CA 92037 USA

[§] Department of Chemistry, The Scripps Research Institute, 10550 North Torrey Pines Road, La Jolla, CA 92037 USA

[‡] Department of Chemical Physiology, The Scripps Research Institute, 10550 North Torrey Pines Road, La Jolla, CA 92037 USA

[#] The Skaggs Institute for Chemical Biology, The Scripps Research Institute, 10550 North Torrey Pines Road, La Jolla, CA 92037 USA

Abstract

The co-crystal X-ray structures of two isomeric α -ketoazole inhibitors (**1** (OL-135) and **2**) bound to fatty acid amide hydrolase (FAAH), a key enzymatic regulator of endocannabinoid signaling, are disclosed. The active site catalytic Ser241 is covalently bound to the inhibitors' electrophilic carbonyl groups, providing the first structures of FAAH bound to an inhibitor as a deprotonated hemiketal mimicking the enzymatic tetrahedral intermediate. The work also offers a detailed view of the oxyanion hole and an exceptional "in-action" depiction of the unusual Ser-Ser-Lys catalytic triad. These structures capture the first picture of inhibitors that span the active site into the cytosolic port providing new insights that help to explain FAAH's interaction with substrate leaving groups and their role in modulating inhibitor potency and selectivity. The role for the activating central heterocycle is clearly defined and distinguished from that observed in prior applications with serine proteases, reconciling the large electronic effect of attached substituents found unique to this class of inhibitors with FAAH. Additional striking active site flexibility is seen upon binding of the inhibitors, providing insights into the existence of a now well-defined membrane access channel with the disappearance of a spatially independent acyl chain-binding pocket. Finally, comparison of the structures of OL-135 (**1**) and its isomer **2** indicates that they bind identically to FAAH, albeit with reversed orientations of the central activating heterocycle, revealing that the terminal 2-pyridyl substituent and the acyl chain phenyl group provide key anchoring interactions and confirming the distinguishing role of the activating oxazole.

Introduction

Endogenous cannabinoids (endocannabinoids) are a class of signaling lipids that include *N*-arachidonoyl ethanolamine (anandamide)¹ and 2-arachidonoyl glycerol (2-AG)², which activate cannabinoid receptors CB1 and CB2 to modulate a range of mammalian behaviors, including pain, inflammation, appetite, motility, sleep, thermoregulation, and cognitive and

*Corresponding Authors: cravatt@scripps.edu, boger@scripps.edu, or stevens@scripps.edu.

emotional states.³ Anandamide and related bioactive fatty acid amides (e.g. oleamide)⁴ (Figure 1) are inactivated by the membrane-bound serine hydrolase fatty acid amide hydrolase⁵ (FAAH).

Preventing the degradation of such endogenous signaling molecules provides an attractive approach for therapeutic intervention that may avoid the side effects associated with direct cannabinoid receptor agonists. Because FAAH blockade only potentiates an activated signaling pathway by raising the endogenous concentration of the released lipid signaling molecule at its site of action, it provides a temporal and spatial pharmacological control that is not typically available to a more classical direct receptor agonist. Extensive research efforts have succeeded in identifying highly potent and selective FAAH inhibitors.⁶ Understanding the mechanism of inhibition for this atypical hydrolytic enzyme from a structural perspective is of central importance.

FAAH belongs to the amidase signature (AS) class of enzymes, a subclass of serine hydrolases that has an unusual Ser-Ser-Lys catalytic triad (Ser241-Ser217-Lys142 in FAAH). FAAH and other AS enzymes also possess a characteristic oxyanion hole, which has an important role in stabilizing intermediates. The catalytic mechanism of FAAH involves the formation of a tetrahedral intermediate, derived from the nucleophilic attack of the catalytic Ser241 residue on the carbonyl group of the substrate. In the case of anandamide, the tetrahedral intermediate collapses to form ethanolamine and the enzyme-bound arachidonoyl-intermediate. Lys142 acts as a general base-general acid during these two events, mediating the deprotonation of Ser241 and the subsequent protonation of the leaving group. Both of these events are coordinated through Ser217, which acts as a proton-shuttle between Lys142 and Ser241. An extensive series of kinetic studies support these distinct roles for Ser241, Ser217, and Lys142 in FAAH catalysis.⁷ The reaction terminates with a water-mediated deacylation of the enzyme-bound acyl-intermediate and release of the free fatty acid (arachidonic acid in the case of anandamide) with restoration of the active enzyme.

In addition to possessing an atypical catalytic core, FAAH bears a series of channels and cavities that are functionally relevant for substrate or inhibitor binding. These include the membrane access channel (MAC), which connects the active site to an opening located at the membrane anchoring face of the enzyme; the cytosolic port that may allow for the exit of hydrophilic products from the active site to the cytosol; and the acyl chain-binding pocket (ABP), which is thought to bind to the substrate's fatty acyl chain during the catalytic reaction.

FAAH hydrolyzes a wide range of both ester and amide substrates with primary amides being hydrolyzed 2-fold faster than ethanolamides.⁸ Although FAAH binds to a large variety of fatty acid chains with various levels of unsaturation and lengths, namely between 7 and 20 carbons,⁹ it preferentially hydrolyzes arachidonoyl or oleoyl substrates (arachidonoyl > oleoyl, 3-fold).⁸ This large structural and size diversity amongst FAAH substrates suggests that the enzyme has developed an effective system to accommodate and bind multiple substrates.

Following early efforts that defined FAAH as a serine hydrolase susceptible to inhibition by substrate-inspired compounds bearing electrophilic carbonyls,¹⁰ we described the development of a series of potent and selective inhibitors enlisting α -ketoheterocycles.¹¹ First introduced by Edwards *et al.* for the inhibition of serine proteases,¹² such inhibitors form reversible covalent tetrahedral adducts with the nucleophilic serine in the enzyme active site.¹³ In our efforts, initiated at a time when there were still only a handful of such α -ketoheterocycle inhibitors disclosed, OL-135¹⁴ emerged not only as a potent and selective lead inhibitor, but also one whose properties were sufficient to provide *in vivo* evidence that FAAH may constitute an exciting, new therapeutic target for the treatment of pain and inflammatory disorders.¹⁵ Among the most extensively characterized FAAH inhibitors disclosed to date,

OL-135 (**1**) exhibits analgesic activity in pain models with efficacies that match those of morphine (at 1–3 mg/kg, intraperitoneal administration), ibuprofen (at 100 mg/kg, intraperitoneal administration), or gabapentin (at 500 mg/kg or 100 mg/kg, oral or intraperitoneal administration, respectively) at administered doses (10–20 mg/kg, intraperitoneal administration) that approach or are lower than those of such common pain medications.¹⁵ Significantly, the analgesic effects are accompanied by increased endogenous levels of anandamide and are observed without the respiratory depression or chronic dosing desensitization characteristic of opioid administration^{15b,16} or the increased feeding, decreased mobility, and reduced motor control characteristic of cannabinoid (CB1) agonist administration.^{15a,17}

Here we present the crystallographic structures of FAAH bound to two α -ketoazazole inhibitors, OL-135 (**1**)¹⁴ and its isomer **2**¹⁸ (Figure 1). The structures offer insights into inhibitor binding and inactivation of a humanized version of the rat FAAH enzyme,^{20b} confirming that Ser241 attacks the electrophilic carbonyl of such inhibitors and providing the first crystal structures of FAAH covalently bound to a deprotonated hemiketal mimicking the tetrahedral intermediate of substrate hydrolysis. Not only do these structures provide an exquisite view of the oxyanion hole and a unique “in-action” depiction of the catalytic mechanism of FAAH, but they suggest a role for the inhibitor heterocycle that is surprisingly distinct from that observed with other serine proteases.^{13,19} Additional, striking active site flexibility is revealed upon binding of the inhibitors, providing insights into the co-existence of a membrane access channel (MAC) and a spatially independent acyl chain-binding pocket (ABP). The observed flexibility revealed in the structures provides an additional view of the rearrangements that the FAAH active site can accommodate for inhibitor binding that are likely also relevant for substrate recognition and catalysis.

Results

The structure of FAAH bound to the α -ketoazazole inhibitors OL-135 (**1**) and **2** have been solved at a resolution of 2.55Å and 1.84Å, respectively. Processing and refinement statistics are given in Table 1. The overall structure of FAAH bound to these two reversible, covalent inhibitors is similar to the previously published structures of FAAH,²⁰ with a root mean squared deviation (RMSD) below 0.4Å when compared pair-wise over 1080 C α atoms in the dimer. The higher resolution of the structures described here allowed us to assign additional solvent molecules and to clarify the conformation of several residues throughout the enzyme. Unbiased electron density maps show the orientation of the inhibitors in the active site, which is covalently bonded to the catalytic Ser241 through a reaction with the carbonyl group of the inhibitor (Figure 2). Additionally, significant changes have been observed in several amino acids forming the substrate recognition cavities of the enzyme. Superposition of the two structures reveals an identical binding mode of **1** and **2**. The following description of the bound inhibitors is divided conveniently into regions corresponding to the detailed interactions of the inhibitor with the channel/pocket network and the catalytic machinery comprising the catalytic core of FAAH, i.e. the oxyanion hole and the catalytic triad.

OL-135 (**1**) and **2** induce a reorganization of the membrane access channel (MAC) and acyl chain-binding pocket (ABP)

The phenethyl portion of the OL-135 adduct extends towards the ABP and MAC, the cavity connecting FAAH's catalytic core to the surface of a membrane-associated region of the protein. Hydrophobic and aromatic residues pack tightly against the inhibitor backbone and phenyl group, forming a cavity complementary in shape to the bound compound. A number of favorable van der Waals interactions are observed with Tyr194, Phe244, Thr377, Leu380, Leu404, Phe432, Thr488, and Val491. The π -system of the phenyl group is engaged with two

aromatic CH- π type interactions with the ring hydrogens of the aromatic residues Phe381 and Phe192. When compared with its orientation in the recently reported FAAH-PF-750 and -PF-3845 structures,^{20a,b} the side chain of Phe192 is tilted about 30 and shifted towards the phenyl group of OL-135 (Figures 2 and 3) in order to provide an improved geometry for the T-shaped interaction to form. Similarly, residue Phe381 slightly changes its conformation to adapt to the phenyl group of the inhibitor in order to provide a proper geometry for the CH- π interaction. It is likely that analogous aromatic CH- π interactions with double bonds stabilize substrate binding of the unsaturated fatty acid substrates, including anandamide and oleamide. A striking example of FAAH's remarkable flexibility is a marked movement of the protein backbone in the vicinity of the catalytic core from amino acid Phe192 to Asp195. This is especially evident when we compare the binding of OL-135 to PF-3845 (Figure 3).^{20a} The reason for this rearrangement may be the presence and positioning of the piperidine group in the PF-750 and PF-3845 structures, which force Ser193 and adjacent amino acids away from the inhibitor, due to van der Waals repulsion forces. It is likely that the bound complex of FAAH with OL-135 more closely resembles the enzyme's conformation in this region as it acts on endogenous substrates.

The residues Phe432, Met436, and Met495 are also characterized by high flexibility, and it appears that they can assume one of two alternative conformations depending on the inhibitor's hydrophobic tail. In the conformation induced by OL-135, residue Phe432 undergoes a complete reorientation, while the two methionines reorient with their sulfur lone pair electrons towards the phenyl hydrogens of the inhibitor, engaging in two aromatic CH- π interactions.²¹ The net result is that the ABP is now completely reorganized, and the MAC remains open and fully expanded. In previously determined structures,²⁰ the channel connecting the enzyme's active site to the membrane-anchoring region of FAAH bifurcates into two hydrophobic cavities, the MAC and the distal portion of the ABP. In the structures presented here, the compound's hydrophobic tail (phenhexyl chain) does not protrude deep into the protein region previously defined as the ABP, rather it binds up to and terminates at the proximal portion of the cavity leading to the membrane. Analysis of the surface profile of the bound OL-135 structure indicates that the rearrangement of residues Phe432, previously proposed to be a dynamic paddle modulating the architecture of the FAAH active site cavities,^{20b} as well as Met436 and Met495 contribute concertedly to a shortening of the ABP and its overall merging with the MAC, which results in a broadening of the distal portion of the latter channel (Figure 4). The FAAH-OL-135 structure is therefore locked in an 'open-channel conformation', similar to that observed in the FAAH-PF-750^{20b} structure, and distinct from the FAAH-MAP^{20c} and FAAH-PF-3845^{20a} structures. The data obtained to date suggest that Phe432, Met436, and Met495 are key residues for substrate sorting among FAAH's active site channels. As discussed below, these residues also appear to provide a key anchoring interaction for binding inhibitors related to OL-135 and may represent key interactions contributing to preferential binding of arachidonoyl and oleoyl chain substrates.

Inhibitor interactions at the cytosolic port revealed

The cytosolic port has the important function of interacting with and stabilizing the leaving group of substrates and inhibitors, as well as potentially providing a channel for water to enter the active site to promote turnover of the acyl-enzyme intermediate. The FAAH crystal structures disclosed thus far have yet to provide insights into this important region of the enzyme.²⁰ In contrast to these previous structures solved with acylating (urea inhibitors, PDB codes 2vya and 2wap) or phosphorylating inhibitors (MAFP inhibitor, PDB code 1mt5), the OL-135 structure provides the first view of an inhibitor that extends into the cytosolic port, and the opportunity to examine the structure in light of extensive efforts that have probed inhibitor-protein interactions in this polar region of FAAH.

The FAAH-OL-135 structure reveals multiple intermolecular and intramolecular interactions. The oxazole and pyridyl rings are quasi-coplanar, with a dihedral angle across the rings of approximately 15°, and oriented in a manner such that the pyridyl nitrogen is directed toward the oxazole aryl CH rather than the oxazole oxygen (*anti* vs. *syn*). This preferred *anti* orientation avoids a destabilizing electrostatic interaction between the electron lone pairs on the pyridyl nitrogen and the oxazole oxygen that accompanies adoption of the alternative *syn* coplanar orientation, while maintaining the stabilizing conjugation between the π -systems of the two aromatic rings. Earlier, high level computational studies suggested there is an energetic torsional energy penalty associated with binding that disrupts their near coplanar pyridine-oxazole arrangement and that the *anti* conformation is significantly more stable.²² The pyridine nitrogen is within hydrogen-bonding distance to a bound water molecule, which is hydrogen bonded to Thr236. In turn, Thr236 is hydrogen bonded to Lys142, which is integral to the Ser241-Ser217-Lys142 catalytic triad. This indirect hydrogen bond to Thr236 may highlight an unappreciated importance of this residue in pre-catalytic binding, since it may serve as an indirect conduit to the key catalytic Lys142 residue and lock the bound pyridine substituent into one possible orientation. Despite the entropic energy penalty resulting from this restraint, the systematic structure-activity relationships defined for this class of FAAH inhibitors and discussed below indicate that there is an offsetting enthalpy gain that provides an overall enhanced stabilization of the complex. Further stabilization is provided by the amino acid Cys269, which undergoes a marked translation of the α -carbon and a side chain rotation of about 140° when compared to the other available structures. This pronounced conformational change results in a reorientation of the thiol group towards the inhibitor, thereby engaging in a sulfur-aromatic interaction with the pyridine ring,²³ suggesting that this residue may also be involved in substrate recognition and binding.

The catalytic core with an enzyme-bound tetrahedral intermediate

The electron density found at the catalytic core unambiguously supports the expectation that OL-135 is a covalent, albeit reversible, inhibitor of FAAH.¹⁴ The electron density indicates that the inhibitor is covalently linked to Ser241 through a tetrahedral carbon (Figure 2), with its oxygen anion strongly coordinated to the oxyanion hole.²⁴ Among the FAAH structures disclosed to date, the OL-135 complex most closely resembles the authentic catalytic tetrahedral intermediate state. In fact and aside from the somewhat related FAAH-MAP structure^{20c}, where the catalytic Ser241 is covalently modified with an uncharged tetrahedral phosphonate, the structure presented in this work is the first containing an oxyanion group that is identical to that of a substrate's tetrahedral intermediate. Even though only minor changes are noted in the oxyanion hole of the structure presented here, we propose an expanded definition of the residues comprising this motif beyond that described in previous work.^{6,20c} More precisely and in contrast to any other serine hydrolase studied thus far, we propose that the oxyanion hole in FAAH is composed of four main chain amide N-H groups, including those of Ile238, Gly239, Gly240, Ser241, as well as secondary interactions provided by the side chains Asp237, Arg243, and Asn498. This latter set of residues forms an additional layer of hydrogen bonds and is tightly connected to the four main chain amide groups. Examination of the available structures reveals that these seven amino acids making up the oxyanion hole have lower B-values, suggesting a strong interaction among them. They exert a potent stabilization effect either directly through a tight hydrogen bond network or through formation of an electrostatic positive hole. Consistent with this view, the oxyanion of bound OL-135 is well coordinated to the four oxyanion hole amide groups through tight hydrogen bonds and/or electrostatic interactions. The distances are 2.8Å, 2.6Å, 3.0Å, and 2.8Å respectively, and are reflective of oxyanion (-O⁻) versus protonated hemiketal (-OH) binding. These can be compared with corresponding distances of 3.0Å, 2.9Å, 3.6Å, and 3.1Å in the FAAH-PF-750 structure taken to represent the acyl-enzyme complex, and 2.5Å, 2.7Å, 3.4Å, and 3.2Å in the rFAAH-MAP structure. In addition to the closer interatomic distances, further changes are

evident from the structure. First, in contrast to the carbonyl oxygen of other inhibitors, the oxyanion in the bound OL-135 is located at the center of the oxyanion hole defined by the backbone amide groups of the amino acids Ile238–Ser241. Second, the carbon–oxyanion axis is accurately aligned perpendicular to the plane of these four amino acids. As a consequence and compared to structures of an acyl–enzyme complex, the γ -oxygen of Ser241 and the bound carbon of the inhibitor are displaced and pulled towards the oxyanion hole (Figure 5). The oxyanion hole itself appears to be undergoing subtle changes in the orientation of the backbone amide groups to improve the geometry for hydrogen-bonding to the oxyanion of OL-135. However, the RMSD between any pair of structures available when calculated over all atoms in the oxyanion hole residues is smaller than 0.5 Å. The more favorable distances observed in the OL-135 complex are therefore the consequence of a difference in oxyanion position and inhibitor penetration into the oxyanion hole rather than protein movement. Overall, it would appear that the interactions of the oxygen atom in OL-135 are especially favorable, consistent with oxyanion stabilization of a tetrahedral intermediate relative to an acyl intermediate.

The last important interaction observed at the catalytic core of the enzyme is mediated by Ser217, a member of the catalytic triad. Rather than lying in the plane of the oxazole and aligned to hydrogen bond to the oxazole nitrogen, this residue is located above and pointing towards the oxazole π -system at a distance of about 3.4 Å to the aromatic centroid and at a distance of 3.1–3.3 Å from the oxazole nitrogen (Figure 2). Similarly, Lys142 is located over 3.5 Å from the oxazole nitrogen and is not spatially aligned for hydrogen bonding. Both residues are also not aligned for conventional hydrogen bonding to the oxazole oxygen (distance of 3.9 Å and 5.4 Å, respectively). This lack of a stabilizing hydrogen bond interaction with the basic nitrogen of the oxazole is in sharp contrast to the role of the heterocycles that was first defined in the pioneering efforts of Edwards *et al.*¹⁹ with the serine protease porcine pancreatic elastase bound to an α -ketobenzoxazole competitive inhibitor. Like the many related serine protease cases that have since been explored,¹³ Edwards *et al.* observed that His57, homologous to Ser217, is hydrogen bonded to the benzoxazole nitrogen, preferentially providing stability to the bound tetrahedral complex. In our case, the Ser217 as well as the Lys142 orientation relative to the oxazole plane seems to preclude the formation of a strong hydrogen bond to the nitrogen and/or oxygen of the oxazole ring. Instead, given its geometry, a Ser217-mediated OH– π hydrogen bond would seem more plausible.²⁵ The effect of this interaction is central to the rationale behind enzyme inactivation and stabilization of the tetrahedral complex with this class of inhibitors. As discussed in detail below, the consequences are that the role of the heterocycle is quite different for FAAH inhibition and this may account for the remarkable and unanticipated substituent effects observed in our work²⁶ relative to those defined by Edwards and others.^{13,19,24} In this regard, it is important to note that prior modeling studies enlisting the use of Monte Carlo simulations in conjunction with free energy perturbation calculations (MC/FEP) projected a Ser217 to oxazole oxygen (not nitrogen) hydrogen bond along with a Lys142 and Thr236 hydrogen-bonding network with the attached pyridine, albeit with a different bound geometry and without the benefit of the inclusion of the bound water molecules.²²

Comparative binding of the isomeric inhibitor 2 relative to OL-135

One key feature to arise from the analysis of the X-ray structure of OL-135 bound to FAAH is the role of the central activating heterocycle. Unlike its behavior in other α -ketoheterocycles that inhibit serine proteases, the oxazole of OL-135 was not found to engage in classical stabilizing hydrogen-bonding interactions that might influence its active site orientation. Rather, its role more simply appears to be to activate the electrophilic carbonyl for addition by Ser241, while providing polar surface area that is buried (solvated) in the bound complex, and serving as the template from which attached substituents may be directed to engage in stabilizing interactions within the active site. With OL-135, this raised the question of whether

the bound orientation of the oxazole or the placement of its pyridine substituent was most important. In preceding studies and at odds with a conventional role of the activating heterocycle, we disclosed a series of results that we suggested could be explained best by invoking a flipped orientation of the central heterocycle in order to maintain an attached substituent interaction at the FAAH active site.^{11,14,18} The most relevant of these examples is the α -keto oxazole **2**,¹⁸ an isomer of OL-135 in which the pyridine substituent is placed at the oxazole C4 versus C5 position. The structure of **2** bound to FAAH was also solved (Figure 6) and the results of its examination are detailed below. Given the overall similarity between the two compounds (OL-135 and **2**), the co-crystal structure of FAAH with **2** also enables a generalized validation of the conclusions drawn from the OL-135 structure. Furthermore, the higher resolution (1.84 Å) and better crystallographic statistics for this structure (Table 1) allows a more reliable analysis of protein conformation, inhibitor binding, and especially the determination of crystallographic water molecules. Like the complex with OL-135, Ser241 was found to be covalently bound to the carbonyl of **2**, producing a tetrahedral intermediate stabilized by alkoxide binding in the oxyanion hole. The most significant feature in the bound structure of **2** is the observation that the pyridine substituent is located precisely at the same site and engaged in the same active site interactions as OL-135, whereas the central activating heterocycle is now flipped by 180° reversing the location of the oxazole nitrogen and oxygen atoms in order to maintain the near coplanar pyridine-oxazole arrangement in an *anti* conformation.²² The fact that the central activating oxazole can flip by 180° without significantly affecting affinity indicates that classical heteroatom hydrogen bonding of the activating heterocycle to core catalytic residues is not significantly contributing to the binding of OL-135 or **2**. The water molecule in the cytosolic port mediating the indirect Thr236 hydrogen bond to the pyridine substituent is even better resolved in this complex. Interestingly and consistent with the FAAH-OL-135 structure, this water molecule is located at a position that would be occupied by the pyridine substituent if the oxazole were bound in the orientation observed with OL-135.²² This reinforces the implications that the interaction of the pyridine substituent with the active site bound water in the cytosolic port may serve a much more fundamental role in stabilizing the binding of OL-135 and **2** to FAAH than one might anticipate at first glance or upon examination of the single structure of bound OL-135. The anchoring interaction of the pyridine substituent complements the similar key anchoring interaction of the phenyl group at the opposite end of the inhibitor bound structure in the MAC. In fact, the disposition of the phenylhexyl chain in the hydrophobic substrate binding pocket is analogous to that observed with OL-135. Importantly and due to the strong interactions with the surrounding residues already described in detail earlier, the terminal phenyl groups from the two structures have been found to exactly overlay with each other (Figure 7). Overall, all of the residue arrangements described in the OL-135 structure find confirmation in this second higher resolution structure, providing essentially identical inhibitor-protein interactions and the presence of an “open-channel conformation” accompanied by fusion of the ABP and MAC.

Discussion

Active site flexibility and binding

The structures of FAAH bound with different inhibitors offer the opportunity to analyze FAAH's active site flexibility, strongly impacting mechanistic and drug design efforts. In contrast to previous studies proposing a structural rigidity of trypsin-like serine proteases,²⁷ it is evident that FAAH is able to adapt to the different chemical nature of inhibitors by exhibiting a rather pronounced flexibility, thus supporting induced fit binding (Figure 3 and 4).

The most significant of the observed flexibility can be found in the MAC and ABP regions. The strategic placement of the phenyl group in proximity to the ABP that is observed in the X-ray structure is consistent with its importance in conveying enhanced potency to the α -

ketoazole inhibitors,^{11,14,26,28} presumably derived from its role in mimicking the π -unsaturation of anandamide ($\Delta^{8,9}$ double bond), oleamide ($\Delta^{9,10}$ double bond) and related fatty acid amide substrates. Surrounding the phenyl-binding region, there is sufficient room and protein flexibility to accommodate the range and character of appended phenyl substituents ($m \geq p > o$) that have been shown to maintain or even enhance the affinity of inhibitors closely related to OL-135.²⁸

The phenyl-binding region appears to constitute a special site at the intersection of the MAC and ABP. Not only do inhibitors that contain a shorter linking methylene chain expectantly exhibit a progressive and substantially reduced affinity for FAAH, but even the α -ketoazole-based inhibitors that extend beyond this site experience a progressive and diminished binding affinity.¹⁴ This is observed even with inhibitors that do not contain the π -unsaturation, suggesting that any major protein reorganization to accommodate the longer inhibitors offsets potential gains in inhibitor binding derived from their increased size (length), whereas the shorter inhibitors simply fail to fully benefit from the forces that stabilize substrate binding. In these studies, the optimal length linking the phenyl ring to the reactive carbonyl was established to be 5–6 methylenes, and this is well reflected in the precise phenyl placement in the crystal structure of bound OL-135 and **2**. Unlike the precise placement of the phenyl group, the structure resolution is insufficient to define the precise conformation of the linking chain and may in fact reflect an averaged conformation. In the case of OL-135 and **2** (6 methylene linkers), the linking chain adopts a bound conformation that embodies at least one gauche turn versus an intrinsically more stable extended conformation. One of these found at C4–C7 most likely is constituting a site that presumably accommodates the anandamide $\Delta^{5,6}$ double bond, while the second is found at C2–C5. The latter is presumably offset by a more favorable accommodation of the anchoring phenyl group in its key binding site. Consistent with the hydrophobic character of the protein in this linking region, introduction of polar atoms into the linker progressively diminish the inhibitor 26,28 potency ($\text{CH}_2 > \text{S} > \text{O} > \text{NMe}, \text{CH}(\text{OH}) > \text{SO} > \text{SO}_2, \text{CONH}$).^{26,28}

An additional significant finding that is highlighted in the FAAH–OL-135 structure are interactions between the ligand's pyridine substituent and residues lining the cytosolic port, including Cys269 and especially the water-mediated hydrogen bond to Thr236. Consistent with this latter observation, replacing the pyridyl nitrogen in OL-135 by a carbon (phenyl vs. 2-pyridyl) reduces the inhibitor potency approximately 20-fold, and even changing the position of the nitrogen within the pyridine ring results in a 3–4-fold loss in potency.¹⁴ In a systematic probe of this effect, the potency of the α -ketoazole-based inhibitors was found to smoothly correlate with the hydrogen bond acceptor properties of the attached C5 heterocycle (e.g. 2-pyridyl = 2-oxazole > 2-thiazole > 2-furan > 2-thiophene > phenyl).¹⁴ Although the origin of the effects of the inhibitors in this region are yet to be fully defined with this related set of X-ray structures, it is of special note that OL-135 (**1**) and **2** clearly benefit from an apparent indirect, and potentially mobile hydrogen-bonding interaction to a residue (Thr236) intimately engaged in the catalytic action of the enzyme. It is not yet clear whether this effect is further enhanced by the catalytic Lys142 hydrogen bond to Thr236. Moreover, it is also not clear whether this water-mediated hydrogen bond to the pyridyl nitrogen is simply serving as a stabilizing active site hydrogen bond or whether it is influencing the inhibitor potency by enhancing the electron-withdrawing character of the pyridyl substituent.²⁶ In this regard and consistent with the importance of the hydrogen bond, it is of note that a systematic exploration of C4 substituents on the pyridine group of OL-135 revealed that inhibitor potency increased, albeit modestly, with the electron-donating properties of the C4 substituent.^{26a} Thus, despite decreasing the intrinsic electron-withdrawing properties of the pyridyl substituent, the inhibitor potency increased with its expected hydrogen bonding trends. What is clear is that this interaction is flexible, potentially accommodating a hydrogen bond acceptor at varied locations,^{11a} that the interaction is sufficiently strong to account for enhanced inhibitor

potencies over well-founded predictions ($-\log K_i$ vs. σ_p),^{18,26} and that it serves as a key anchoring interaction that predominates even over the central heterocycle orientation. Unlike the irreversible carbamate and urea based inhibitors that do not maintain binding interactions with the cytosolic port, not only is it possible to enhance the affinity and selectivity²⁹ of the reversible α -ketoazazole inhibitors through key interactions in this unique polar region of the enzyme active site, but modulation of their physical (e.g. solubility) and PK properties may be best addressed by modification in this region of the inhibitors.²⁶

Role of the central activating heterocycle

Expectations were that upon Ser241 addition to the reactive carbonyl with conversion of the electron-withdrawing ketone to a tetrahedral intermediate, the oxazole nitrogen would become more basic and capable of engaging in stronger hydrogen bonding interactions.¹² This preferential stabilization of the tetrahedral adduct was anticipated to be derived from hydrogen bonding with the active site Ser217, extended in turn by Lys142 hydrogen bonding and mimicking the protonation of the substrate leaving group. Inconsistent with these expectations, inhibitor potency actually increases,^{26c} not decreases, with the addition of electron-withdrawing substituents on the oxazole that would be expected to preclude or diminish such a stabilizing hydrogen bonding interaction. True to these observations and in contrast to prior precedent, the heterocycle's role is not one of preferential hydrogen bonding between its basic nitrogen and core catalytic residues to stabilize the tetrahedral adduct. Rather and since the structure of bound OL-135 and **2** lack any direct, stabilizing hydrogen bonding between FAAH and the inhibitors' oxazole, its role appears to be more intimately related to the intrinsic electron-withdrawing character of the central heterocycle enhanced by its attached substituents serving to activate the reactive carbonyl for nucleophilic attack. This newly appreciated role of the central activating heterocycle³⁰ of the α -ketoazazole inhibitors of FAAH reconciles the electronic role the attached substituents play and validates the observation that their effects are extraordinarily large ($\rho = 3-3.4$ in a Hammett analysis).^{18,26b,c}

Inactivation mechanism

Upon binding to FAAH, the carbonyl group of OL-135 (**1**) undergoes nucleophilic attack by the catalytic Ser241. In contrast to the physiological substrates, where both protonation via the Lys142-Ser217 proton transfer network and the release of electrons to the substrate's leaving group upon collapse of the oxyanion are coupled to the same atom, the enzyme-bound tetrahedral intermediate of OL-135 cannot protonate and release a leaving group. Rather, Ser217 is engaged in a hydrogen bond with the oxazole π -ring and cannot donate the proton to the oxazole C2 carbon (Scheme 1).

In other words, the protonation is uncoupled to the generation of the leaving group and the reaction cannot proceed further. Therefore, Ser241 remains covalently, but reversibly modified, and the resulting complex can be viewed as a trap of the tetrahedral intermediate state of FAAH. The proposed Ser217- π hydrogen bond likely stabilizes binding of this class of highly potent inhibitors in the FAAH active site, and could not be predicted in our previous work²² and has not been observed in prior structural studies of α -keto heterocycle complexes with serine proteases.¹³ Since this tetrahedral adduct mimics a key interaction for substrate binding and catalysis by FAAH, it may represent a dominant hydrogen bond stabilizing the binding of this class of inhibitors. Upon Ser241 addition to the reactive carbonyl with conversion of the electron-withdrawing ketone to a tetrahedral intermediate, the oxazole nitrogen and aromatic ring become more basic and therefore better at engaging in a stronger hydrogen bonding interaction. Because of the differential strength of the Ser217 hydrogen bond to the oxazole π -system, extended by Lys142 hydrogen bonding to Ser217 and mimicking the protonation of the substrate leaving group, it conceivably could preferentially stabilize the

tetrahedral intermediate versus the carbonyl bound state of the inhibitor and substantially contribute to their unique potency for FAAH.

A prominent role in complex stabilization is exerted by the oxyanion hole. The stabilization effect of the oxyanion hole not only contributes to catalytic efficiency and inhibition potency, but may affect the substrate and inhibitor specificity of the enzyme. We analyzed and compared other serine hydrolase structures, in particular the other two AS enzyme structures malonamidase E2 (MAE2, PDB codes 1gr9 and 1grk)³¹ and peptide amidase (PAM, PDB code 1m21),³² and found that the FAAH–oxyanion hole system is distinct amongst this large class of enzymes. Indeed, whereas no Arg243 is found in the homologous region of PAM, the MAE2 structure shows how this arginine has shifted an amino acid position and plays structural- and charge-stabilization roles of the substrate's carboxylic acid group from a different location of the active site.³³ Additionally, Asp237 is conserved in the PAM but not in the MAE2 structures, and a corresponding residue for Asn498 is not present in either structures. The much more elaborated oxyanion hole system in FAAH potentially allows enhanced stabilization of the negative charge in the enzyme-bound tetrahedral intermediate state, thereby contributing to the exceptional potency of the α -ketoheterocycles, the unique selectivity of urea inhibitors, and the higher reactivity toward fluorophosphonates.^{7b}

Conclusion

The membrane-bound serine hydrolase FAAH is an emerging drug target with important potential medicinal applications, ranging from the treatment of pain to anxiety. In the past years, extensive drug discovery efforts have led to the identification of several classes of inhibitors that block enzymatic activity and resulted in a marked augmentation of endocannabinoid levels in various tissues including those found in the central and peripheral nervous systems. The covalent, reversible inhibitor OL-135 (**1**) is the most prominent member in a class of potent and selective inhibitors based on an α -ketoheterocycle scaffold that has shown to be pharmacologically efficacious *in vivo* for the treatment of pain. In this work, we have presented co-crystal structures of FAAH with OL-135 (**1**) and **2**, an isomer in which the 2-pyridine substituent is attached at C4 instead of C5 to the central oxazole. Detailed analysis that explains binding features and inactivation mechanisms including novel insights into key stabilizing interactions of the protein–inhibitor complex has been provided. Together with confirming the covalent addition of Ser241 to the inhibitor electrophilic carbonyl providing a bound deprotonated hemiketal mimicking the enzymatic tetrahedral intermediate, the structures capture the exquisite oxyanion hole and atypical catalytic residues in a key intermediate state and clearly define the role of the inhibitors' activating central heterocycles. Of additional interest are the interactions revealed in the region of the cytosolic port, information that has been hindered in previously published structures due to the intrinsic properties of other classes of inhibitors. Furthermore, extensive active site reorganization has been noted in the presented structures, a feature that is likely at the basis of substrate recognition and relocation within the active site during catalysis. The knowledge gathered will aid future drug design efforts and in the understanding of substrate degradation.

Materials and Methods

FAAH expression and purification

The *N*-terminal transmembrane-deleted (Δ TM) truncated form (amino acids 30–579) of the humanized/rat (h/r) FAAH gene cloned into a pET28a vector was used for heterologous expression in the *E. coli* strain BL21 A.I. (Invitrogen). The h/rFAAH construct is characterized by mutations resulting in the replacement of six amino acids to the rFAAH protein sequence (L192F, F194Y, A377T, S435N, I491V, V495M) in order to recreate the binding profile of the human enzyme.^{20b} The protein was purified as previously described.^{20a,b} In brief, three

chromatography steps including metal affinity, cation exchange, and size exclusion chromatography were utilized to reach a purity greater than 95% as visualized from Coomassie blue staining gel electrophoresis (not shown). In contrast to previous purification procedures, the detergent used in the last two steps of purification was 0.08% *n*-undecyl- β -D-maltoside (Anatrace). Protein concentrations were determined by using a reducing-agent compatible BCA protein assay kit (Pierce Biotechnology).

Synthesis of inhibitors, OL-135 (1) and 2

The inhibitors were prepared according to published literature procedures.^{14,18}

Crystalization and crystal structure determination

The protein sample was concentrated to 25–30 mg/mL in a buffer containing 10 mM Hepes (pH 7.0), 500 mM NaCl, 0.08% *n*-undecyl- β -D-maltoside, and 2 mM dithiothreitol. The additives xylitol (Sigma) and benzyldimethyl(2-dodecyloxyethyl)-ammonium chloride (Aldrich) were supplemented to the protein sample up to a concentration of 12% and 1%, respectively. After mixing 1:1 the protein solution to the crystallization buffer (30% PEG400, 100mM Hepes pH 7.5, and 100 mM NaCl), 6% dimethyl formamide (DMF) and 0.5 mM inhibitor (in DMF) were added to obtain the final crystallization mother liquor. Crystals were grown by sitting-drop vapor diffusion at 14 °C in 96-well plates (Innovaplate SD-2; Innovadyne Technologies) and frozen by plunging into liquid nitrogen directly after harvesting. The data for the co-crystal structure of FAAH with OL-135 (1) were collected at a temperature of 100 K from a single crystal at Stanford Synchrotron Radiation Laboratory (SSRL, Menlo Park, CA, USA) on beamline 11-1 (λ :0.97945Å). The data for the FAAH–2 structure were collected at the GM/CA-CAT beamline of the Advanced Photon Source (APS, Argonne, IL, USA) by using a 10- μ m beam collimator (λ :1.03320Å). Data were processed using XDS package.³⁴ Structures were solved and refined by using programs contained in the CCP4 package.³⁵ The software suite Phenix³⁶ was used to refine individual atomic displacement parameters. Results from data processing and structure refinement are provided in Table 1. The two crystal lattices of FAAH–OL-135 and FAAH 2 were found in the P3₂21 and P2₁, respectively, containing a FAAH dimer in the asymmetric unit. The structures were determined at a resolution of 2.55Å (OL-135) and 1.84Å (2) and solved by molecular replacement using the coordinates of the FAAH–PF-750 structure (PDB code: 2vya) as a search model. Chemical parameters for the inhibitors were calculated by the Dundee PRODRG web server.³⁷

Acknowledgments

We thank Michael S. McCormick for helpful discussions in the structure refinement and Katya Kadyshkevskaya for the help with graphics. We gratefully acknowledge the financial support of the National Institutes of Health (DA017259 and DA015648) and the Skaggs Institute for Chemical Biology. Portions of this research were carried out at the Stanford Synchrotron Radiation Lightsource, a national user facility operated by Stanford University on behalf of the U.S. Department of Energy, Office of Basic Energy Sciences. The SSRL Structural Molecular Biology Program is supported by the Department of Energy, Office of Biological and Environmental Research, and by the National Institutes of Health, National Center for Research Resources, Biomedical Technology Program, and the National Institute of General Medical Sciences. Use of the Advanced Photon Source at Argonne National Laboratory was supported by the U. S. Department of Energy, Office of Science, Office of Basic Energy Sciences, under Contract No. DE-AC02-06CH11357.

References

1. Devane WA, Hanus L, Breuer A, Pertwee RG, Stevenson LA, Griffin G, Gibson D, Mandelbaum A, Etinger A, Mechoulam R. *Science* 1992;258:1946–9. [PubMed: 1470919]
2. Sugiura T, Kondo S, Sukagawa A, Nakane S, Shinoda A, Itoh K, Yamashita A, Waku K. *Biochem Biophys Res Commun* 1995;215:89–97. [PubMed: 7575630]

3. (a) Calignano A, La Rana G, Giuffrida A, Piomelli D. *Nature* 1998;394:277–81. [PubMed: 9685157] (b) Labar G, Michaux C. *Chem Biodivers* 2007;4:1882–902. [PubMed: 17712824] (c) Karanian DA, Bahr BA. *Curr Mol Med* 2006;6:677–84. [PubMed: 17022737]
4. (a) Cravatt BF, Prospero-Garcia O, Siuzdak G, Gilula NB, Henriksen SJ, Boger DL, Lerner RA. *Science* 1995;268:1506–9. [PubMed: 7770779] (b) Cravatt BF, Lerner RA, Boger DL. *J Am Chem Soc* 1996;118:580–590. (c) Boger DL, Henriksen SJ, Cravatt BF. *Curr Pharm Des* 1998;4:303–314. [PubMed: 10197045]
5. Cravatt BF, Giang DK, Mayfield SP, Boger DL, Lerner RA, Gilula NB. *Nature* 1996;384:83–7. [PubMed: 8900284]
6. Seierstad M, Breitenbucher JG. *J Med Chem* 2008;51:7327–43. [PubMed: 18983142]
7. (a) Patricelli MP, Cravatt BF. *J Biol Chem* 2000;275:19177–84. [PubMed: 10764768] (b) McKinney MK, Cravatt BF. *Annu Rev Biochem* 2005;74:411–32. [PubMed: 15952893] (c) Patricelli MP, Lovato MA, Cravatt BF. *Biochemistry* 1999;38:9804–12. [PubMed: 10433686] (d) Patricelli MP, Cravatt BF. *Biochemistry* 1999;38:14125–30. [PubMed: 10571985]
8. Boger DL, Fecik RA, Patterson JE, Miyauchi H, Patricelli MP, Cravatt BF. *Bioorg Med Chem Lett* 2000;10:2613–6. [PubMed: 11128635]
9. Patricelli MP, Cravatt BF. *Biochemistry* 2001;40:6107–15. [PubMed: 11352748]
10. (a) Patterson JE, Ollmann IR, Cravatt BF, Boger DL, Wong CH, Lerner AE. *J Am Chem Soc* 1996;118:5938–45. (b) Boger DL, Sato H, Lerner AE, Austin BJ, Patterson JE, Patricelli MP, Cravatt BF. *Bioorg Med Chem Lett* 1999;9:265–70. [PubMed: 10021942]
11. (a) Boger DL, Sato H, Lerner AE, Hedrick MP, Fecik RA, Miyauchi H, Wilkie GD, Austin BJ, Patricelli MP, Cravatt BF. *Proc Natl Acad Sci USA* 2000;97:5044–9. [PubMed: 10805767] (b) Boger DL, Miyauchi H, Hedrick MP. *Bioorg Med Chem Lett* 2001;11:1517–20. [PubMed: 11412972] (c) Leung D, Du W, Hardouin C, Cheng H, Hwang I, Cravatt BF, Boger DL. *Bioorg Med Chem Lett* 2005;15:1423–8. [PubMed: 15713400]
12. Edwards PD, Bernstein PR. *Med Res Rev* 1994;14:127–94. [PubMed: 8189835]
13. Maryanoff BE, Costanzo MJ. *Bioorg Med Chem* 2008;16:1562–95. [PubMed: 18053726]
14. Boger DL, Miyauchi H, Du W, Hardouin C, Fecik RA, Cheng H, Hwang I, Hedrick MP, Leung D, Acevedo O, Guimarães CR, Jorgensen WL, Cravatt BF. *J Med Chem* 2005;48:1849–56. [PubMed: 15771430]
15. (a) Lichtman AH, Leung D, Shelton CC, Saghatelian A, Hardouin C, Boger DL, Cravatt BF. *J Pharmacol Exp Ther* 2004;311:441–8. [PubMed: 15229230] (b) Chang L, Luo L, Palmer JA, Sutton S, Wilson SJ, Barbier AJ, Breitenbucher JG, Chaplan SR, Webb M. *Br J Pharmacol* 2006;148:102–13. [PubMed: 16501580] (c) Palmer JA, Higuera ES, Chang L, Chaplan SR. *Neuroscience* 2008;154:1554–61. [PubMed: 18541380] (d) Schlosburg JE, Boger DL, Cravatt BF, Lichtman AH. *J Pharmacol Exp Ther* 2009;329:314–23. [PubMed: 19168707]
16. Bailey CP, Connor M. *Curr Opin Pharmacol* 2005;5:60–8. [PubMed: 15661627]
17. Varvel SA, Bridgen DT, Tao Q, Thomas BF, Martin BR, Lichtman AH. *J Pharmacol Exp Ther* 2005;314:329–37. [PubMed: 15831444]
18. DeMartino JK, Garfinkle J, Hochstatter DG, Cravatt BF, Boger DL. *Bioorg Med Chem Lett* 2008;18:5842–6. [PubMed: 18639454]
19. Edwards PD, Meyer EFJ, Vijayalakshmi JA/TP, Andisik DA, Gomes B, Strimpler A. *J Am Chem Soc* 1992;114:1854–1863.
20. (a) Ahn K, Johnson DS, Mileni M, et al. *Chem Biol* 2009;16:411–20. [PubMed: 19389627] (b) Mileni M, Johnson DS, Wang Z, Everdeen DS, Liimatta M, Pabst B, Bhattacharya K, Nugent RA, Kamtekar S, Cravatt BF, Ahn K, Stevens RC. *Proc Natl Acad Sci USA* 2008;105:12820–4. [PubMed: 18753625] (c) Bracey MH, Hanson MA, Masuda KR, Stevens RC, Cravatt BF. *Science* 2002;298:1793–6. [PubMed: 12459591]
21. (a) Reid KSC, Lindley PF, Thornton JM. *FEBS Lett* 1985;190:209–13. (b) Zauhar RJ, Colbert CL, Morgan RS, Welsh WJ. *Biopolymers* 2000;53:233–48. [PubMed: 10679628]
22. Guimarães CR, Boger DL, Jorgensen WL. *J Am Chem Soc* 2005;127:17377–84. [PubMed: 16332087]
23. Duan G, Smith VHJ, Weaver DF. *Mol Phys* 2001;99:1689–99.

24. (a) Edwards PD, Zottola MA, Davis M, Williams J, Tuthill PA. *J Med Chem* 1995;38:3972–82. [PubMed: 7562931] (b) Edwards PD, Andisik DW, Bryant CA, Ewing B, Gomes B, Lewis JJ, Rakiewicz D, Steelman G, Strimpler A, Trainor DA, Tuthill PA, Mauger RC, Veale CA, Wildonger RA, Williams JC, Wolanin DJ, Zottola M. *J Med Chem* 1997;40:1876–85. [PubMed: 9191965]
25. Steiner T, Koellner G. *J Mol Biol* 2001;305:535–57. [PubMed: 11152611]
26. (a) Romero FA, Du W, Hwang I, Rayl TJ, Kimball FS, Leung D, Hoover HS, Apodaca RL, Breitenbacher JG, Cravatt BF, Boger DL. *J Med Chem* 2007;50:1058–68. [PubMed: 17279740] (b) Kimball FS, Romero FA, Ezzili C, Garfinkle J, Rayl TJ, Hochstatter DG, Hwang I, Boger DL. *J Med Chem* 2008;51:937–47. [PubMed: 18247553] (c) Romero FA, Hwang I, Boger DL. *J Am Chem Soc* 2006;128:14004–5. [PubMed: 17061864]
27. Guvench O, Price DJ, Brooks CL 3rd. *Proteins* 2005;58:407–17. [PubMed: 15578663]
28. Hardouin C, Kelso MJ, Romero FA, Rayl TJ, Leung D, Hwang I, Cravatt BF, Boger DL. *J Med Chem* 2007;50:3359–68. [PubMed: 17559203]
29. Leung D, Hardouin C, Boger DL, Cravatt BF. *Nat Biotechnol* 2003;21:687–91. [PubMed: 12740587]
30. Garfinkle J, Ezzili C, Rayl TJ, Hochstatter DG, Hwang I, Boger DL. *J Med Chem* 2008;51:4392–403. [PubMed: 18630870]
31. Shin S, Lee TH, Ha NC, Koo HM, Kim SY, Lee HS, Kim YS, Oh BH. *EMBO J* 2002;21:2509–16. [PubMed: 12032064]
32. Labahn J, Neumann S, Buldt G, Kula MR, Granzin J. *J Mol Biol* 2002;322:1053–64. [PubMed: 12367528]
33. Yun YS, Lee W, Shin S, Oh BH, Choi KY. *J Biol Chem* 2006;281:40057–64. [PubMed: 17077089]
34. Kabsch W. *J Appl Cryst* 1993;26:795–800.
35. COLLABORATIVE COMPUTATIONAL PROJECT, NUMBER 4. *Acta Cryst* 1994;D50:760–3.
36. Adams PD, Grosse-Kunstleve RW, Hung LW, Ioerger TR, McCoy AJ, Moriarty NW, Read RJ, Sacchettini JC, Sauter NK, Terwilliger TC. *Acta Cryst* 2002;D58:1948–54.
37. Schuettelkopf AW, van Aalten DMF. *Acta Cryst* 2004;D60:1355–1363.

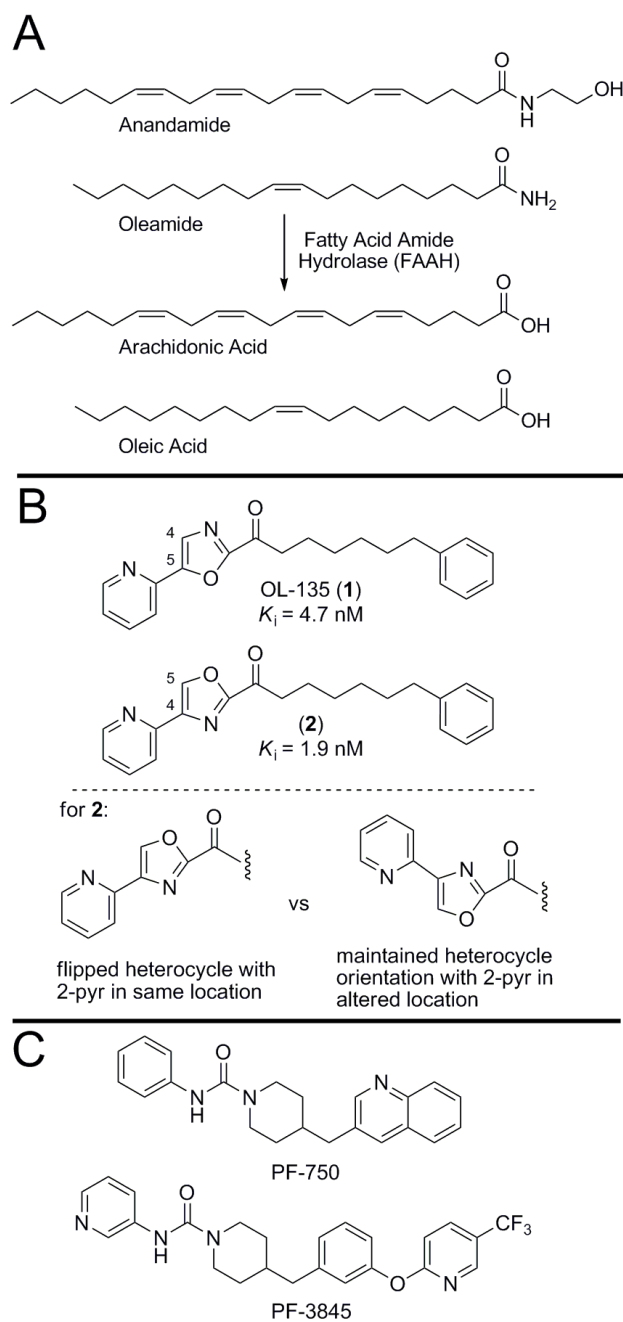


Figure 1.
A) Endogenous substrates and their inactive enzymatic products. B) Two α -ketooxazole inhibitors of FAAH, **1** (OL-135) and **2**. C) Two urea inhibitors of FAAH, PF-750 and PF-3845.

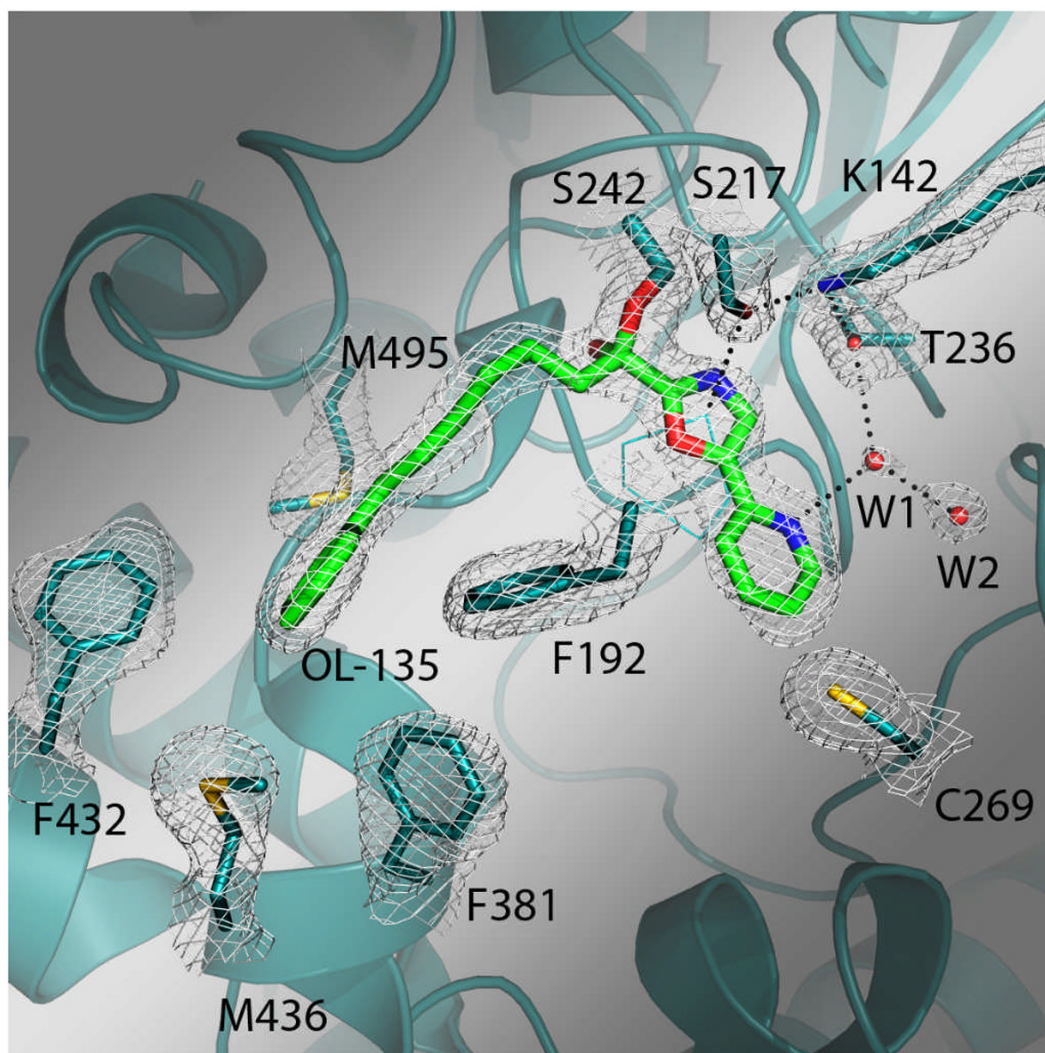


Figure 2. FAAH active site with bound OL-135 (in green). The protein backbone is shown in dark green ribbon representation. The density at 1.2 σ contour is shown in white mesh.

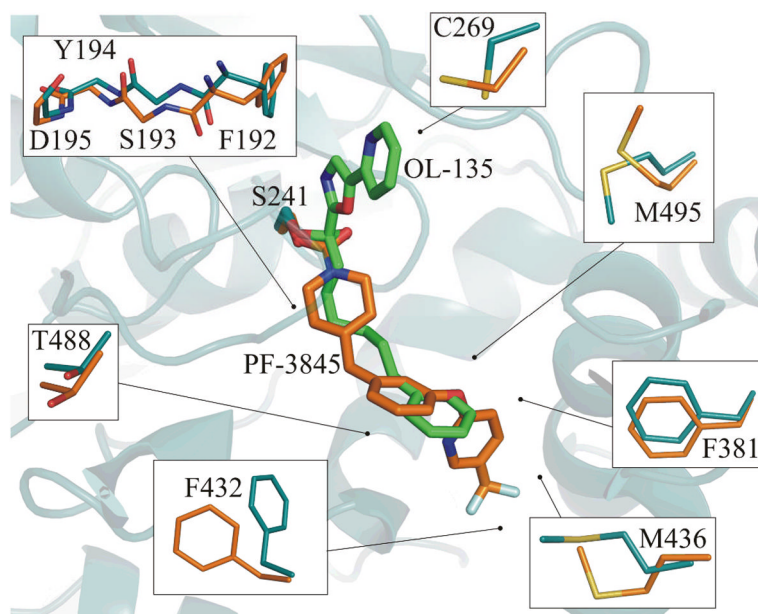


Figure 3. Protein flexibility at the active site. The FAAH–PF-3845 structure (PDB code 2wap) is shown in orange, whereas the OL-135–FAAH structure is shown in green.

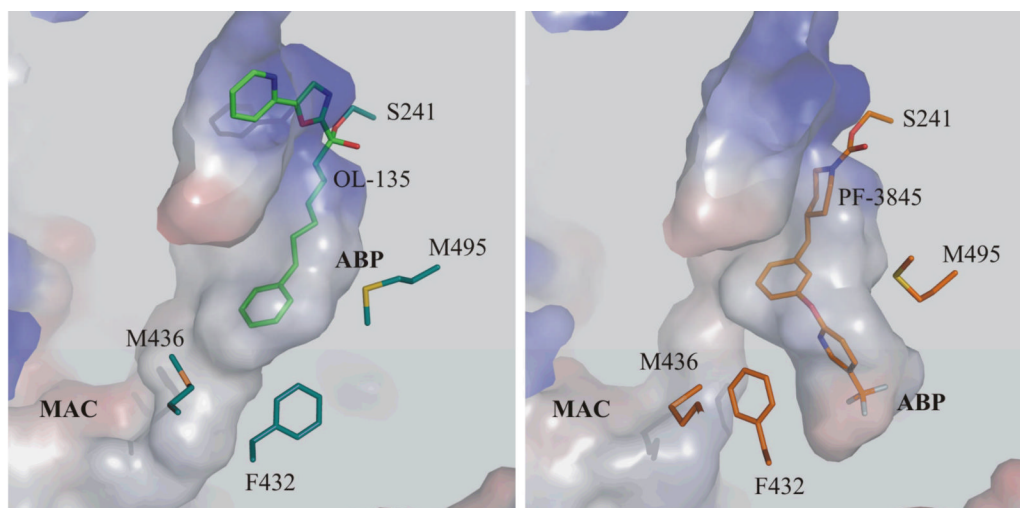


Figure 4. Reorganization of the acyl chain-binding pocket. Open (left) and closed (right) membrane access channel. The distal portion of the acyl chain-binding pocket is absent with bound OL-135 (left), but present in the PF-3845 structure (right). Surface representation of the FAAH-OL-135 and FAAH-PF-3845 structures are shown. PF-3845 and FAAH residues are shown in orange (right); OL-135 and FAAH residues are shown in green and dark green, respectively.

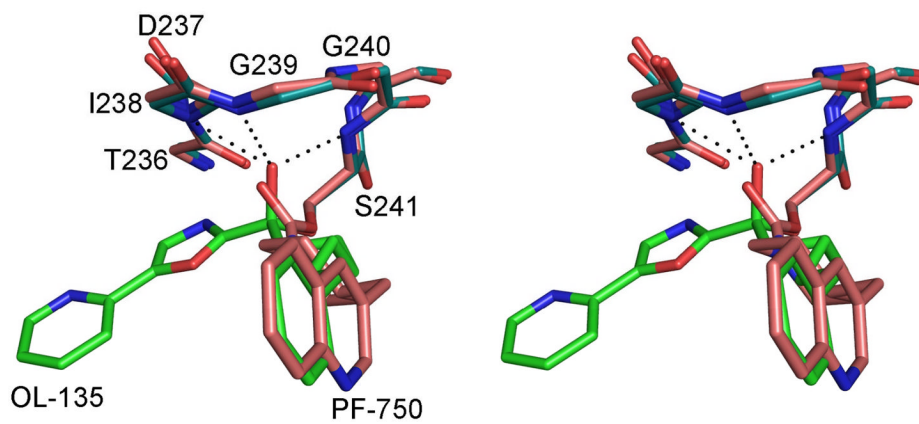


Figure 5. Stereo view of the OL-135 (green sticks) oxyanion interacting with the oxyanion hole and superposition with the FAAH-PF750 structure (pink sticks).^{20b}

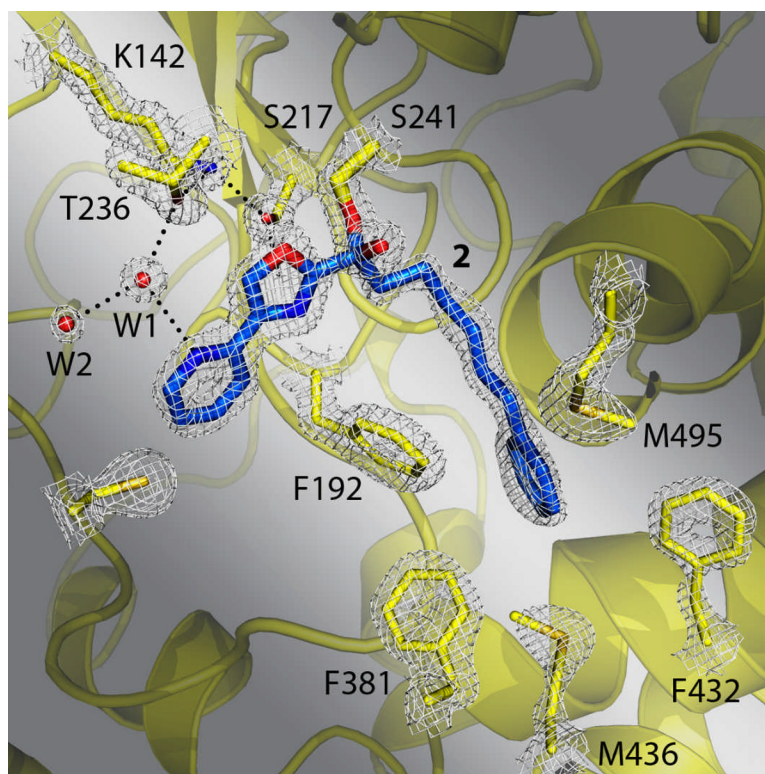


Figure 6. FAAH active site with bound inhibitor **2** (in blue). The protein backbone is shown in yellow ribbon representation. The density at 1.8σ contour is shown in white mesh.

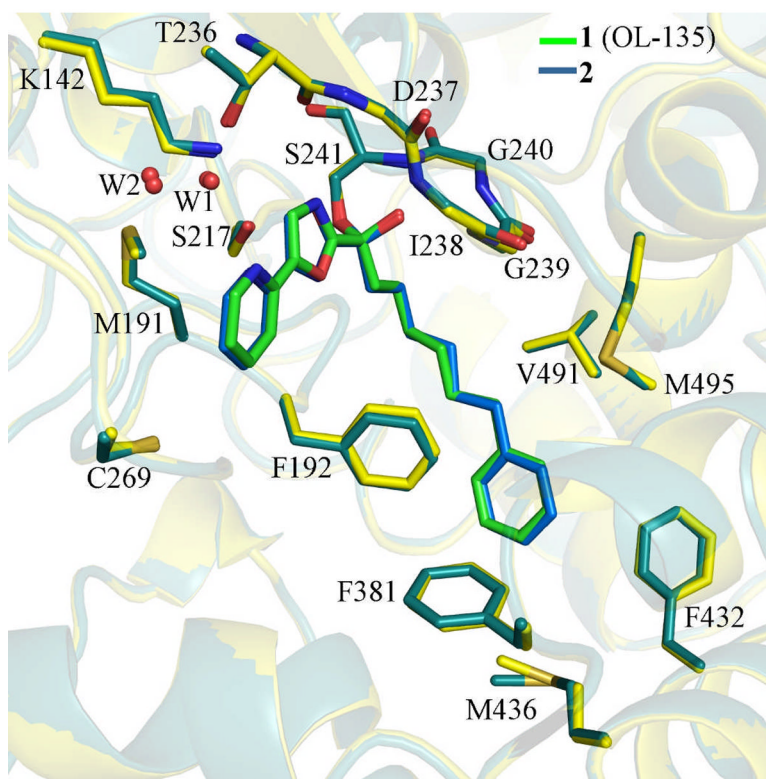
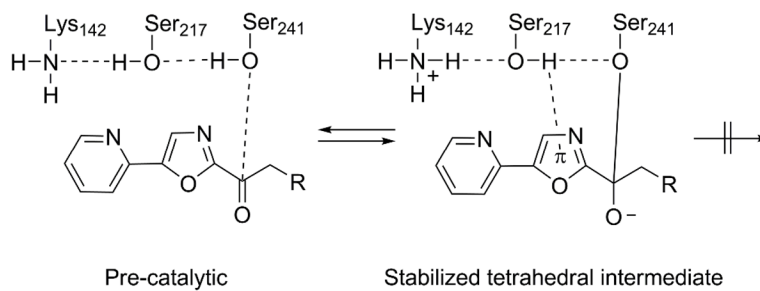


Figure 7. Binding mode and superposition of the co-crystal structures with compound **1** and **2**. The inhibitors **1** and **2** are shown in green and blue, respectively. The backbone of the protein structures are shown in yellow (**1**) and dark green (**2**).



Scheme 1.
 α -Ketooxazole inhibition of FAAH.

Table 1
Crystallographic statistics: data collection and refinement statistics.

	1 (OL-135)	2
Data collection		
Space group	P3 ₂ 21	P2 ₁
Cell dimensions		
<i>a</i> , <i>b</i> , <i>c</i> (Å)	103.44, 103.44, 254.13	75.83, 106.21, 79.39
α , β , γ (°)	90, 90, 120	90, 100.20, 90
Resolution (Å)	30-2.55(2.62-2.55)	30-1.84(1.90-1.84)
<i>R</i> _{merge} (%)	16.1(68.1)	10.3(62.4)
<i>I</i> / σI	9.24(2.30)	8.73(2.11)
Completeness (%)	99.6(99.9)	99.1(99.5)
Redundancy	4.3(4.3)	3.7(3.7)
Refinement		
Resolution (Å)	2.55(2.60-2.55)	1.84(1.86-1.84)
No. reflections	52071	106195
<i>R</i> _{work} / <i>R</i> _{free} (%)	18.4(21.4)/23.5(26.8)	18.6(23.8)/21.4(26.3)
No. atoms	8668	9083
Protein	8431	8407
Ligand/ion	51	51
Water	186	625
<i>B</i> -factors	25.9	30.0
Protein	25.9	29.5
Ligand/ion	27.3	24.6
Water	24.8	36.1
R.m.s. deviations		
Bond lengths (Å)	0.014	0.014
Bond angles (°)	1.450	1.469